Improving Channel Capacity in Indoor 4 × 4 MIMO Base Station Utilizing Small Bidirectional Antenna

Bakar Rohani, *Member, IEEE*, Kanata Takahashi, Hiroyuki Arai, *Fellow, IEEE*, Yasuko Kimura, and Taisuke Ihara

***Abstract*—Preparing toward the new-generation communication by improving the capacity in the channel can be achieved by employing a MIMO system with polarization diversity means. This paper presents a low-profile 4 × 4 MIMO bidirectional antenna consisting of two composite antennas mounted on a ground plane. The composite antenna is constructed by stacking a notch antenna and a loop antenna on top of each other and each antenna is fed independently. This antenna is capable of dual-polarized radiation patterns pointing in two different directions, where the notch antenna produces a horizontally polarized wave in the *x*-axis direction while the loop antenna gives a vertically polarized wave in the *y*-axis direction. The combination of two composite antennas has good isolation between the elements and is capable of improving the channel capacity for indoor MIMO base station applications. This paper includes the validation of both the fabrication of the proposed antenna design and the channel propagation measurement using the proposed antenna, confirming the excellent antenna performance for long term evolution application at a frequency of 3.5 GHz.**

***Index Terms*—Bidirectional, channel capacity, dual polarization, loop antenna, low profile, MIMO antenna, notch antenna.**

I. Introduction

A NEW generation of mobile wireless technology speaks of lower latency and more capacity than current wireless communication. Approaching the future wireless network, the antenna design and propagation characteristics must work efficiently in the existing frequency while at the same time preparing toward the new-generation challenges such as low cost, easy installation, intelligent design as well as practical implementation [1], [2]. The multiple-input multiple-output (MIMO) system is one notable solution in enhancing channel capacity for an indoor base station [3]–[5]. MIMO antennas in indoor environment utilized few parameters such as polarization, radiation pattern, and array configuration in order to improve the capacity in the channel [6]–[8]. Polarization diversity technique has been proven can increase the capacity in the channel, where in [9] the antenna with different polarization is capable of more capacity than the antenna with the same polarization. Similar result also was obtained where the hybrid polarization system has been proven give more capacity than the single polarization system [7]. Following these trends, more studies have been done on utilizing the polarization diversity technique effectively while keeping the antenna design as low profile as possible without reducing the capacity [10], [11]. On the other hand, delivering unique radiation pattern comes almost complementary with the configuration of the antenna array itself. An optimized radiation pattern can be achieved by adjusting the parasitic elements of the antenna array [12] or by adding slot or cavity in the structure [11], thus improving the antenna performance especially in capacity aspect.

Practical implementation and optimum performance has to be delivered, however, in designing MIMO antenna as the structure usually is in array configuration. A low profile, small in size design has to be considered to maintain a low-cost antenna with simple installation. Unfortunately, constructing an array in small size is not one easy task. The mutual coupling between the antenna elements must be kept as low as possible, maintaining a low correlation coefficient between the arrays. Favorably, however, utilizing polarization diversity technique with directional radiation pattern notably demonstrates low correlation coefficient with higher capacity than the conventional antenna such as dipole antenna [13], [14]. This paper focus on designing a low-profile design consists of simple element and small size enough for indoor base station application utilizing the polarization diversity technique to improve the capacity of the MIMO antenna channel. The challenge is to develop a structure that not only has low-profile design in structure and dual-polarization pattern in radiation, but also with high-isolation characteristic between the elements.

In this paper, a low-profile bidirectional antenna composing of vertical and horizontal polarization elements is proposed. In the initial stage, a composite antenna employing both polarization elements is developed keeping good performances in both S-parameter and radiation pattern. Then, two composite antennas are combined together by mounting them on the same ground plane to produce the dual-polarization characteristic in both x-axis and y-axis directions of the structure. The bidirectional antenna is suitable for a wide area line-of-sight (LOS) channel environment targeting the long term evolution application for indoor MIMO base station

Manuscript received January 25, 2017; revised June 12, 2017; accepted October 17, 2017. Date of publication November 9, 2017; date of current version January 2, 2018. This work was supported by YNU. *(Corresponding author: Bakar Rohani.)*

B. Rohani, K. Takahashi, and H. Arai are with the Department of Electrical and Computer Engineering, Yokohama National University, Yokohama 240-8501, Japan (e-mail: rohani-bakar-ng@ynu.ac.jp; takahashi-kanata-zt@ynu.jp; arai-hiroyuki-vk@ynu.ac.jp).

Y. Kimura and T. Ihara are with the Radio Access Network Development Department, NTT DOCOMO, Inc., Yokosuka 239-3586, Japan (e-mail: kimurayas@nttdocomo.com; taisuke.ihara.rd@nttdocomo.com).

Color versions of one or more of the figures in this paper are available online at http://ieeexplore.ieee.org.

Digital Object Identifier 10.1109/TAP.2017.2771951

which operates at frequency 3.5 GHz. The proposed antenna is simulated in MWS software [15].

The organization of this paper is as follows. Following the introduction in Section I, Section II presents the design and the configuration of the proposed antenna and the simulation result of the antenna performance. Then, channel capacity is discussed in Section III, where the theory and the implementation of channel capacity simulation are described in detail. The capacity of dipole antenna, monopole antenna and bidirectional antenna is compared and the improvement in capacity is shown. Section IV presents the performance of the fabricated antenna comparing with the simulation result while channel propagation measurement also is carried out using the fabricated antenna for the validation purpose. And finally in Section V, conclusions are drawn summarizing the study presented in this paper.

II. Antenna Design

Initial stage of proposing the antenna design discusses a simple low-profile structure, but with the radiation pattern in two different directions. The design then is promoted to dual-polarized patterns radiating in both directions. In this section, a composite antenna which is the basic structure is discussed first, following by the examination of a four-element antenna which is the combination of the two composite antennas, combined together on a bigger ground plane producing the 4×4 MIMO bidirectional antenna as the final design.

A. Basic Design of the Composite Antenna

The basic structure of the proposed antenna is adopted so as to produce the output radiation in two different directions. The bidirectional structure which is called a composite antenna utilizes two elements of a simple notch antenna and a loop antenna where each antenna radiates horizontally and vertically polarized wave, respectively. The configuration of the composite antenna is constructed by mounting the loop antenna of 7 mm in height and 37 mm in length on the center of a 200 mm square ground plane. Then, the notch antenna is fixed on top of the loop antenna giving the overall height of the structure of 10.8 mm. While the loop antenna is formed using just simple wire, the notch antenna is constructed using a 0.8 mm substrate with dielectric property of 2.6. Two notches are formed at the bottom side of the substrate providing the notch element for the antenna in the shape of H-pattern. The positioning and configuration of the structure is optimized using characteristic mode analysis as presented in [16]. The notch element is excited by the microstrip line designed in the shape of S-pattern at the top side of the substrate. The shape of the microstrip line provides a reverse excitation to the notch element forcing the current to flow in the opposite side of the notch element. Therefore, the current distributed in y-axis direction is canceled out producing a strong radiation pattern in x-axis direction instead. Fig. 1 shows the composition of the composite antenna in top view and side view as well as details dimension of the structure.

Each element in the composite antenna is fed independently and the feeding points are labeled as Port 1 and Port 2 for the

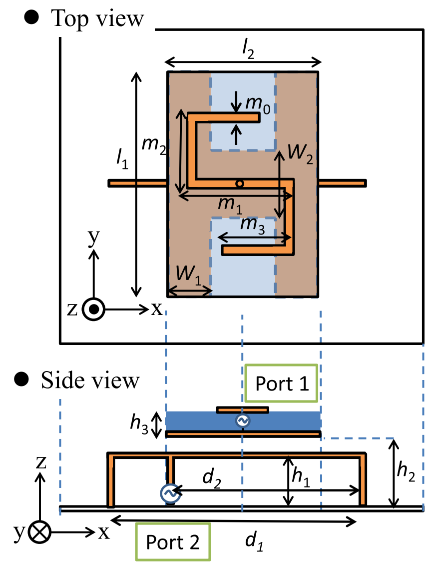

Fig. 1. Structure of the composite notch–loop antenna in top view and side view. [$W_1 = 3, W_2 = 6.5, l_1 = 35.5, l_2 = 19, h_1 = 7, h_2 = 10, h_3 = 0.8, m_0 = 1, m_1 = 17, m_2 = 7, m_3 = 11.5, d_1 = 37$, and $d_2 = 33$ (mm).]

notch antenna and loop antenna, respectively. The optimization of the structure is done for the resonance frequency of 3.5 GHz with the impedance matched at below −10 dB for both elements. The isolation between elements is very good where S_{12} reads at below −30 dB and two radiation patterns in two different directions are obtained. The notch antenna which is excited through Port 1 radiates a strong pattern in x-axis direction with no radiation in yz plane while inversely for the loop antenna which is excited through Port 2, the pattern radiates strongly in y-axis direction instead with no radiation in xz plane. During the fabrication process, however, a problem regarding the feeding point arises where the feeding point for the notch antenna coincides with the loop antenna structure which makes the fabrication process becomes difficult. Therefore, for easy fabrication purpose, the feeding point for the notch antenna has to be changed to a new position that is possible to fabricate while maintaining the good performance of the antenna in both S-parameter and radiation pattern.

B. Design Improvement of the Composite Antenna

An improvement of the design is constructed to address the fabrication issue regarding the feeding point of the notch antenna in the initial design. The dimension of the loop antenna structure is maintained as previously as the performance of the antenna is already good. The design of the notch antenna, however, is changed where the feeding point originally at the center is moved toward the edge of the substrate. At the same time, the size of the substrate is increased adapting the length of the loop antenna. Fig. 2 shows the final design of the improved structure where a new pattern for the microstrip line is formed accommodating the new position of the feeding point. On the other hand, the shape of the notch element is also modified to ensure the ground portion of the microstrip line while at the same time maintaining the symmetrical arrangement of the structure.

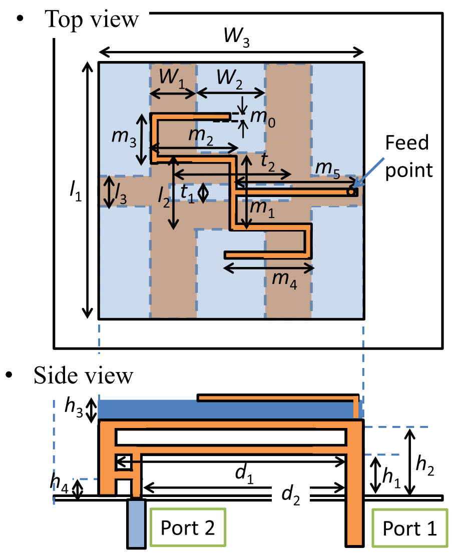

Fig. 2. Final structure of the composite antenna in top view and side view. [$W_1 = 5$, $W_2 = 9$, $W_3 = 46$, $l_1 = 34.75$, $l_2 = 8$, $l_3 = 3$, $h_1 = 8$, $h_2 = 13$, $h_3 = 0.8$, $h_4 = 3$, $m_0 = 0.8$, $m_1 = 7$, $m_2 = 8$, $m_3 = 2.5$, $m_4 = 15.5$, $m_5 = 22$, $d_1 = 41$, $d_2 = 38$, $t_1 = 3.5$, and $t_2 = 13.5$ (mm).]

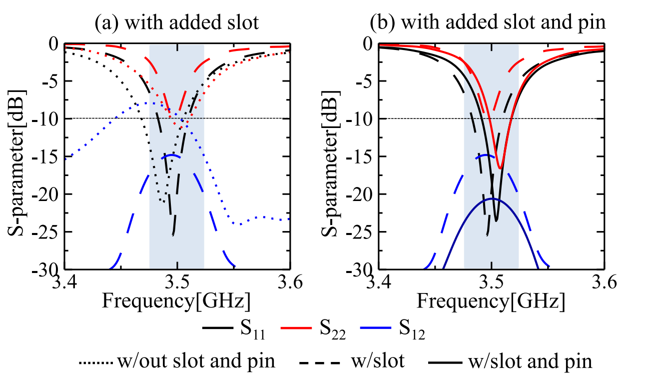

Fig. 3. Comparison of the S-parameter results for the improved design between before and after added slot and short pin. (a) With added slot. (b) With added slot and pin.

Two new adjustments are added to the structure; a short pin and a slot, due to the poor antenna performance especially in term of the S-parameter. Dotted line in Fig. 3(a) shows the S-parameter results without the added slot and short pin and while the S_{11} for the loop antenna is good at -20 dB, the impedance matched for loop antenna (S_{22}) is not very good at -10 dB while the isolation between the elements (S_{12}) is also very poor at 7 dB. The isolation problem is fixed by creating a slot at the center of the notch element as shown in the top view in Fig. 2 where the S_{12} is lowered to -15 dB as presented by the dashed line in Fig. 3. On the other hand, the S_{11} for the loop antenna becomes higher to more than -10 dB, thus a short pin is added to the structure as shown in the side view in Fig. 2. The final design improves not only the S_{11} to below -15 dB but the isolation between the elements is further improves to more than 20 dB. Fig. 3(a) shows the S-parameter comparison between without added slot and short pin and with added slot only, while Fig. 3(b) shows the comparison between with added slot only and with added slot and short pin.

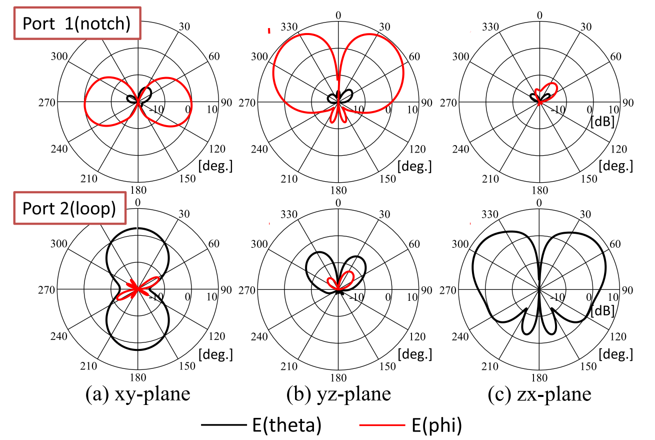

Fig. 4. Radiation patterns of the improved design for Port 1 (notch antenna) and Port 2 (loop antenna) in (a) *xy*, (b) *yz*, and (c) *zx* planes.

The radiation pattern for each element is presented in Fig. 4 in *xy, yz,* and *zx* planes. The radiation pattern in *xy* plane describes that the notch antenna radiates a strong horizontally polarized wave in x-axis direction and the loop antenna radiates a strong vertically polarized wave in y-axis direction. The cross-polarization patterns are within the acceptable range for both elements. The bandwidth obtained initially for Port 1 and Port 2, respectively, is 28 and 20 MHz, which are quite small and needs to be improved to at least 40 MHz while keeping the height of the structure as low as possible. Therefore, in the final design, the height of the loop antenna and the notch antenna is increased to 8 and 13 mm, respectively, producing the final bandwidth value of 47 and 40 MHz, correspondingly.

It is very important to keep the antenna performances especially in term of bidirectional patterns hence the symmetrical arrangement of the structure as the output patterns are very sensitive to the design. The final design of the composite antenna is optimized with the best possible performance including the low coupling between the elements making it possible to extend the design with more elements for MIMO base station antenna application.

C. Final Design of the MIMO Antenna

A two-element composite antenna produces either horizontal or vertical polarization radiation pattern in each x-axis and y-axis direction. To implement the dual-polarization patterns in both directions, a four-element configuration is constructed using the final composite design. Two composite antennas are mounted on a bigger ground plane, arranged diagonally away from each other due to the optimization of the current distribution. In [16], the positioning of two composite antennas is discussed confirming that the current distribution of each composite antenna is less affected when arranged diagonally away. Fig. 5 shows the four-element structure where the distance from the center of each composite antenna is fixed at 0.75 λ. The feeding for the notch elements and the loop elements are labeled as Ports 1 and 3 and Ports 2 and 4, respectively. Similar antenna performances are achieved for

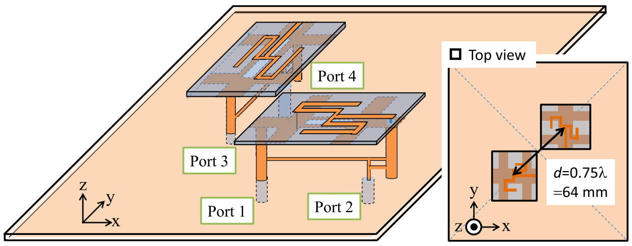

Fig. 5. Four-element bidirectional structure. (Notch antenna: Port 1 and Port3. Loop antenna: Port 2 and Port 4.)

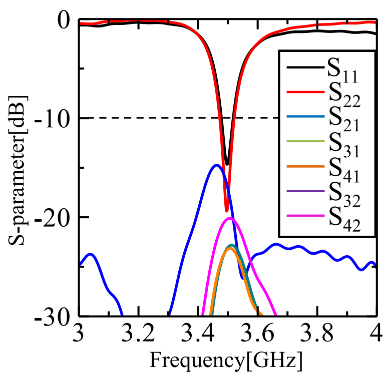

Fig. 6. S-parameter results of the four-element bidirectional antenna.

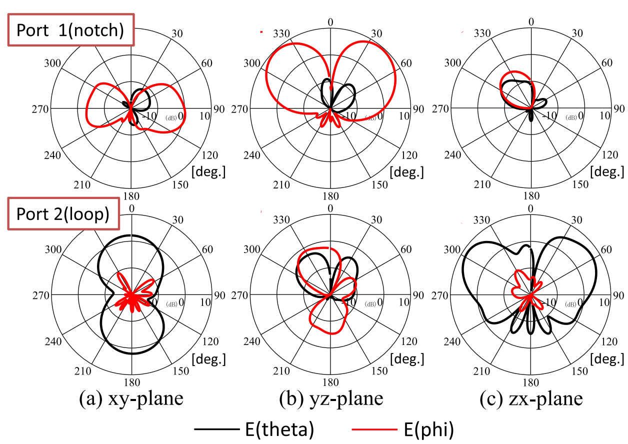

Fig. 7. Radiation patterns of the antenna for Port 1 (notch antenna) and Port 2 (loop antenna) in (a) *xy*, (b) *yz*, and (c) *zx* planes.

each composite antenna, thus only the results for Port 1 and Port 2 are shown for easier explanation. Figs. 6 and 7 show the antenna performance results of the four-element bidirectional antenna. The S_{11} for notch antenna and S_{22} for loop antenna are -15 and -19 dB, respectively. The lowest isolation result is at 17 dB for S_{21}, but very good results are achieved for S_{31} and S_{41} at -23 dB and S_{32} and S_{42} at -30 and -20 dB, respectively. The radiation patterns show similar results as the composite structure in Fig. 4 verifying the stability of the performance obtained from this design. The cross polarizations increase a little bit as compared to previous results. And as the arrangement of the composite antennas are perpendicular to each other, both horizontally and vertically polarized radiation patterns are achieved in each x-axis and y-axis direction.

III. Channel Capacity

The performance of MIMO system can be evaluated in term of the capacity in the channel where the channel capacity can be represented by numerical value in b/s/Hz. Channel capacity is defined as the maximum amount of information that can be transferred over a communication channel per unit time. In multistreams MIMO system, the channel capacity C is given by the following equation [17]

$$C = \log_2\left(\det\left(I + \frac{\rho}{N_t} H_n H_n^H\right)\right) \tag{1}$$

where I is an identity matrix, ρ is the average SNR at each receiving antenna, and N_t denotes the number of transmitting antennas. The channel response matrix H is referred to a matrix consisting of impulse responses between transmits and receives antenna elements.

A. Channel Capacity Calculation Modeled by Ray Tracing Method for Channel Response Matrix H

According to (1), the capacity in MIMO system is calculated based on the channel response matrix, H. This matrix containing impulse responses between transmit antenna and receive antenna elements is obtained from the simulation process modeled according to ray tracing method. In multipath propagation environment, the signals transmitted from the transmit antenna are reflected, scattered or diffracted by the obstacles before reaching the receive antenna. Ray tracing method is a method of tracking the trajectory of these transmitted signals. There are two types of ray tracing method, named as ray launching method and ray imaging method where the amount of calculations as well as the estimation accuracy for each of these types is different. The evaluation in this research adopts the ray launching method where large numbers of signals are emitted in all directions from the transmission point and the transmission, reflection and diffraction is computes iteratively. The number of the signals transmitted is increased so as sufficient accuracy can be achieved. When the transmitted signals hit the obstacles, losses due to reflection and transmission coefficient at interference are according to Fresnel equation [18].

A close-spaced room with neither door nor window is created in EEM-RTM software [19] without taking into account the thickness of the wall, with the propagation environment set according to ray launching method. All the walls, floors, and ceilings are made of concrete with typical electrical properties as follows: dielectric constant of vacuum $\varepsilon_0 = 8.854 \times 10^{-12}$, dielectric constant $\varepsilon_r = 6.76$, conductivity $\sigma = 0.0023$, and relative permeability $\varepsilon_r = 1$. The simulation parameters for the channel capacity calculation are shown in Table I. An LOS environment is assumed where there is no an object or obstacle aside from transmit and receive antennas inside the room. The maximum reflection time is set to 5 and neither diffraction nor scattering is taken into consideration during simulation process.

B. Simulation Environment and Results

The simulation environment for channel capacity calculation is created in EEM-RTM software visualizing the indoor

TABLE I
SIMULATION PARAMETERS FOR CHANNEL CAPACITY CALCULATION

Channel modelling	Ray Tracing
Number of Tx/Rx Antennas	4 x 4
Carrier Frequency	3.5 GHz
Element spacing of transceiver	0.5λ
Noise Power	5 dB
Transmission Power	- 85 dB
Number of Reflections	5
Receive Antenna	Omnidirectional
Wall characteristics Relative Permittivity Conductivity	Concrete 6.76 0.0023 S/m

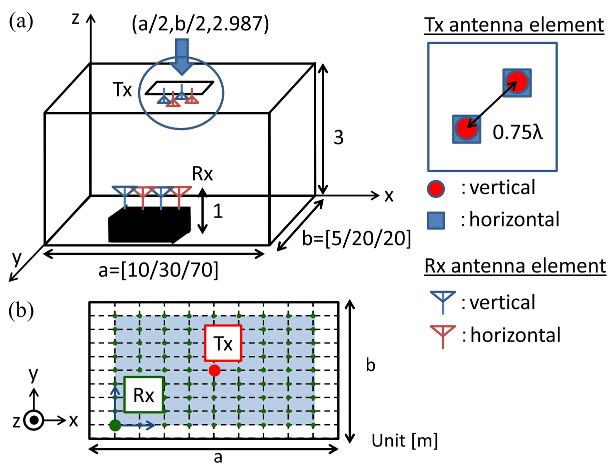

Fig. 8. (a) Simulation environment and (b) transmit and receive antenna configuration for channel capacity simulation.

propagation environment in the MIMO system. Three rooms which different in size are created for comparison purpose, with the smallest named as room A, and the biggest as room C. The height z of all rooms is set at 3 m, while the width x and the length y are set as the following in [x, y, z]: room A [10, 5, 3], room B [30, 20, 3], and room C [70, 20, 3]. The illustration of the room is shown in Fig. 8(a). All the rooms are set in rectangle shape with x-axis longer than y-axis to demonstrate the influence of the different in dimension. Four-element transmit antenna is fixed at 0.013 m from the ceiling while a total of 81 points of four-element receive antennas are positioned 1 m from the floor, shown as the green dots in Fig. 8(b). As the total number of receiving points are the same in all rooms regardless of the size, the distance in x and y of each point in each room is divided equally. The channel capacity is calculated at these 81 points providing the average capacity of the whole room.

On the other hand, four antennas are used at each transmit and receive point assuming 4 × 4 MIMO systems where each point consists of two vertically polarized and two horizontally polarized antennas. The receive antennas are arranged alternatingly with $\lambda/2$ apart in distance and each has omnidirectional radiation pattern. Table II shows the capacity calculation results where for comparison purpose, two situations with and without the presence of the ground plane is considered.

TABLE II
CHANNEL CAPACITY COMPARISON IN b/s/Hz

Room Size	10 x 5 x 3	30 x 20 x 3	70 x 20 x 3
Dipole	29.789	18.197	12.827
Bi-directional	31.05	18.67	13.73
Monopole on ground plane	35.00	22.17	16.02
Bi-directional on ground plane	37.55	22.48	16.23

In the first case without the ground plane, the bidirectional antenna is compared with a dipole antenna while in the second case with the ground plane, the bidirectional antenna is compared with the monopole antenna. In the first step, all the related antennas are simulated in the MWS software to produce their respective radiation patterns for each antenna. In the case of the bidirectional antenna, the radiation pattern is obtained from the proposed antenna in this paper which will be described in Section III. Next, the patterns are called into the EEM-RTM software, simulated and their transmission trajectories are traced for channel response calculation. The output channel response which in matrix form is then inputted in MATLAB program for channel capacity calculation in b/s/Hz.

In the first case without the ground plane, the capacity for bidirectional antenna has higher capacity than dipole antenna in all room sizes including in the biggest room C. In the second case where the ground plane is considered to suppress the radiation toward the ceiling, the overall capacity improves considerably higher than without the ground plane. In this case also the capacity for bidirectional antenna shows much higher capacity than monopole antenna, especially in the smallest room A. In overall, the capacities for bidirectional antenna are higher in all rooms for both cases confirming that the capacity of an indoor environment can be improved by using MIMO system utilizing a directional antenna with polarization diversity technique.

IV. FABRICATION AND EXPERIMENTAL RESULTS

A. Fabrication of the Prototype Antenna

In order to verify the simulation results, the four-element bidirectional antenna is fabricated and measured. The loop elements are constructed using simple wire and a copper plate is used as the ground plane. The notch elements are constructed using R-4737 substrate of 0.8 mm in height. In the initial process, the two-element composite antenna is fabricated first to confirm the dimension of the fabricated structure is matched at the resonance frequency as in the simulation. After confirming the impedance is matched as well as the bidirectional radiation pattern, the four-element antenna is fabricated next.

The measurement process of the fabricated antenna is done for both the reflection characteristic and the radiation pattern to be compared to the simulation results described in Section III. Fig. 9 shows the comparison of the S-parameter results between the simulation and the measurement results for the proposed antenna. The solid line presents the simulation results while the dashed line describes the

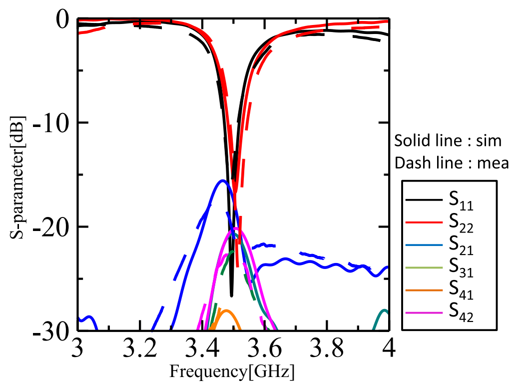

Fig. 9. Comparison between simulation and measurement of the S-parameter results for the four-element bidirectional antenna.

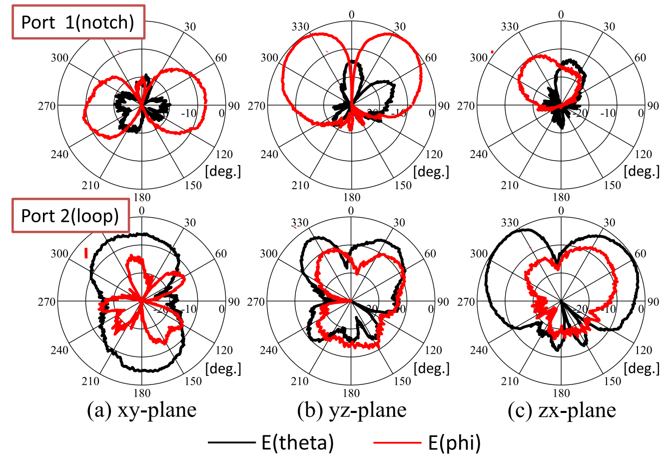

Fig. 10. Measurement results of the radiation patterns for Port 1 (notch antenna) and Port 2 (loop antenna) in (a) *xy*, (b) *yz*, and (c) *zx* planes.

measurement results. The notch antennas are fed by the Port 1 and Port 3 while the loop antennas are fed by Port 2 and Port 4. Comparing the measurement results with the simulation results, the impedance matching for both notch antenna (S_{11}) and loop antenna (S_{22}) are very good at below -10 dB. The isolations between the elements are also very good with the highest reading for S_{21} is -15 dB and all the other readings are below -20 dB. The measurement results are in total agreement with the simulation results which is very favorable especially the isolation between the elements as it is very difficult to fabricate the elements in small size.

The radiation patterns for the measurement results are shown in Fig. 10 in *xy, yz,* and *zx* planes with only Port 1 of notch antenna and Port 2 of loop antenna results are shown as the other ports give similar radiation patterns. For the notch antenna, the pattern radiates strongly in x-axis direction. Comparing to the simulation results in Fig. 7, the radiation in *zx* plane for measurement result is slightly different but it is still within the acceptable range. In other planes, the measurement results are in agreement with the simulation results. Similarly for the loop antenna, the measurement results are comparable with the simulation results for all planes. However, the cross polarizations are slightly bigger in the measurement results due to the difficulty in fabrication. Overall, both horizontally and vertically polarized radiation patterns are achieved in both x-axis and y-axis directions. The top and side views of the fabricated antenna are shown in Fig. 11.

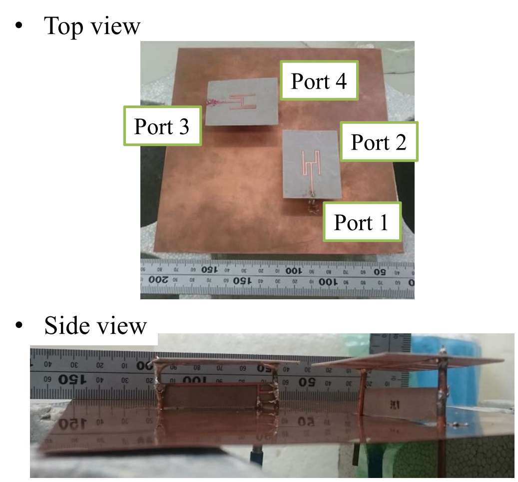

Fig. 11. Top and side views of the fabricated antenna.

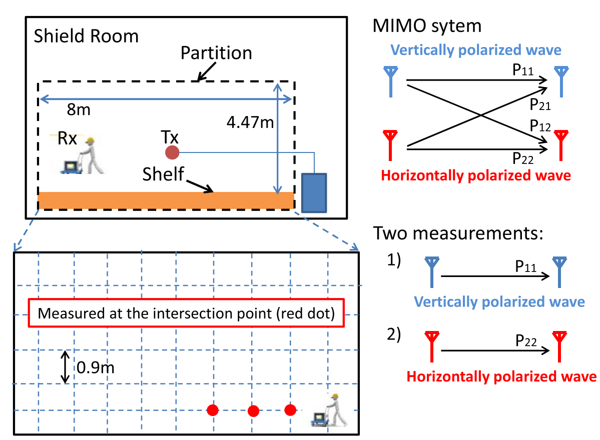

Fig. 12. Propagation environment in the shield room used for radio channel measurement.

B. Channel Propagation Measurement

The measurement of the channel propagation is carried out as the validation for real-world channel measurement and the improvement of the capacity is shown by comparing the proposed antenna with the conventional omnidirectional antenna. The propagation environment is shown in Fig. 12, where one section in the shield room is used for the measurement process. The partition is divided into 45 points of equal length shown in red dots and the received power is measured at each intersection points. The transmitting antenna is located at the upper center of the room which can transmit both vertically and horizontally polarized wave. Two types of receiving antennas are used, the omnidirectional antenna as the conventional antenna and the proposed bidirectional antenna for the comparison purpose. Two cases study is carried out where in Case 1, the direction of the radiation for bidirectional antenna is in y-direction while in Case 2, the direction is in x-direction. Both vertically and horizontally polarized wave

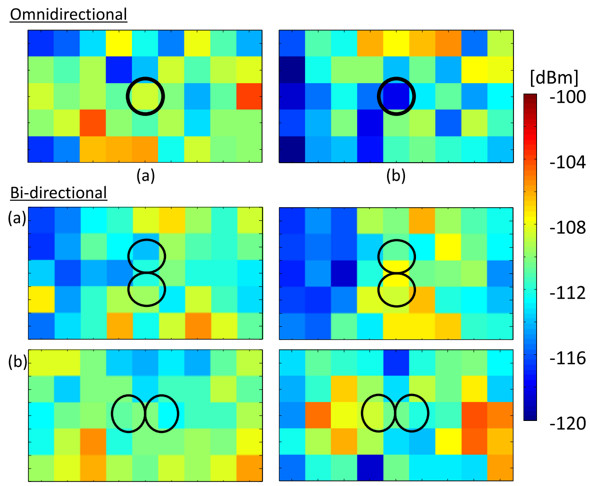

Fig. 13. Received power distribution in the propagation room for (a) vertically polarized wave antenna and (b) horizontally polarized wave antenna.

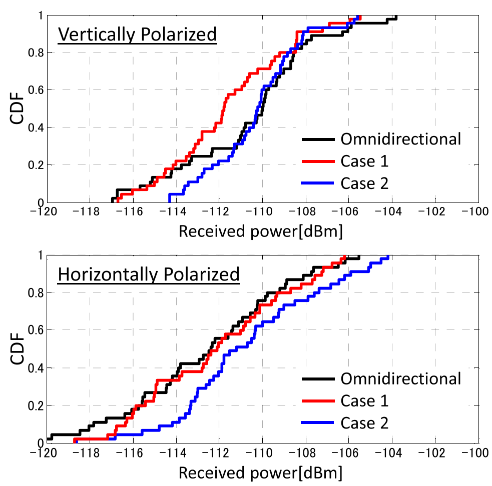

Fig. 14. Cumulative probability distribution of received power.

are measured and the results of the received power are shown in the form of received power distribution map of the area and cumulative probability distribution (CDF) as shown in Figs. 13 and 14, respectively.

The received power distribution maps show that for omnidirectional antenna, the reception level drops largely at the corners and edges of the room in both cases. On the other hand, while the reception level for bidirectional antenna is lower in the null direction of the radiated wave, the reception level is higher than the omnidirectional antenna at the corners and edges. Comparing with the omnidirectional antenna, it can be concluded that the bidirectional antenna that radiates strongly in the longitudinal direction has a distribution in which the reception level is higher than the omnidirectional antenna. The CDF result for vertically polarized wave measurement shows that the area that receives higher level of received power (-108 to -104 dBm) is comparable for all antennas, but for middle level (-112 to -108 dBm), the bidirectional antenna of both cases cover more area than omnidirectional antenna. Furthermore, the area that has the lowest level for bidirectional antenna in Case 2 receives significantly higher power level (-114 to -112 dBm) as compared to the other two measurement (-116 to -114 dBm), with the omnidirectional antenna has area that receives the lowest power level. Meanwhile for the horizontally polarized wave measurement, the CDF result shows that the bidirectional antenna in Case 2 receives marginally highest level of received power in all area with the omnidirectional antenna has the lowest received power area. Thus, it can be concluded that the area in which the reception level is low is considerably less for bidirectional antenna comparing with the omnidirectional antenna. From these results, it is confirmed that the proposed bidirectional antenna provides higher capacity than conventional omnidirectional antenna and effective as MIMO base station antenna with enhanced capacity.

V. Conclusion

In this paper, we proposed a composite antenna consisting of notch antenna and loop antenna mounted on top of each other on a ground plane. The notch antenna produces a horizontally polarized radiation pattern in x-axis direction while the loop antenna produces a vertically polarized radiation pattern in y-axis direction. This composite antenna then is combined together on a bigger ground plane, arranged diagonally away from each other producing dual-polarized radiation pattern in both x-axis and y-axis directions. The impedances are matched at below -10 dB at the resonance frequency of 3.5 GHz with the lowest isolation between all the elements is at 15 dB. The measurement results for the S-parameter results are in total agreement with the simulation results. And although the simulation results for the radiation patterns are slightly better than the measurement results due to the difficulty in fabrication, it is still within the acceptable range. The similarity of the results of each element for both composite antennas shows the stability of the structure while maintaining the low isolation between the elements. The channel propagation measurement also shows that good results have been obtain where the proposed antenna has a distribution in which the reception level is higher than the conventional omnidirectional antenna. It is confirmed that the proposed antenna is effective to enhance the capacity propagation the channel. As a result, a four-element dual-polarized bidirectional MIMO antenna with a small structure of 13.8 mm in height intended for indoor base station with enhanced capacity capability is obtained.

Acknowledgment

The authors would like to thank all the editorial effort which made the paper more readable. The authors would also like to thank the valuable comments of the reviewers and the associate editor.

References

[1] D. Muirhead, M. A. Imran, and K. Arshad, “A survey of the challenges, opportunities and use of multiple antennas in current and future 5G small cell base stations,” *IEEE Access*, vol. 4, pp. 2952–2964, 2016.

[2] M. Benisha, R. T. Prabu, and V. T. Bai, “Requirements and challenges of 5G cellular systems,” in *Proc. 2nd Int. Conf. Adv. Elect., Electron., Inf., Commun. Bio-Inform.*, 2016, pp. 251–254.

[3] M. Matthaiou, A. M. Sayeed, and J. A. Nossek, “Maximizing LoS MIMO capacity using reconfigurable antenna arrays,” in *Proc. Int. ITG Workshop Smart Antenna (WSA)*, 2010, pp. 14–19.

[4] K. Cho and Y. Inoue, "Influence of cross-polarization characteristics on indoor MIMO performance using a dual-polarized base station antenna," in *Proc. IEEE Int. Symp. Antennas Propag. (APSURSI)*, Jul. 2010, pp. 1–4.
[5] P. Wang, H. Wang, L. Ping, and X. Lin, "On the capacity of MIMO cellular systems with base station cooperation," *IEEE Trans. Wireless Commun.*, vol. 10, no. 11, pp. 3720–3731, Nov. 2011.
[6] N. Honma, K. Nishimori, R. Kudo, Y. Takatori, T. Hiraguri, and M. Mizoguchi, "A stochastic approach to design MIMO antenna with parasitic elements based on propagation characteristics," *IEICE Trans. Commun.*, vol. E93-B, no. 10, pp. 2578–2585, 2010.
[7] P. Kyritsi, D. C. Cox, R. A. Valenzuela, and P. W. Wolniansky, "Effect of antenna polarization on the capacity of a multiple element system in an indoor environment," *IEEE J. Sel. Areas Commun.*, vol. 20, no. 6, pp. 1227–1239, Aug. 2002.
[8] T. Mitsui, M. Otani, C. H. Y. Eugene, K. Sakaguchi, and K. Araki, "Indoor MIMO channel measurements for evaluation of effectiveness of array antenna configurations," in *Proc. IEEE VTC-Fall*, vol. 1. Oct. 2003, pp. 84–88.
[9] P.-Y. Qin, Y. J. Guo, and C.-H. Liang, "Effect of antenna polarization diversity on MIMO system capacity," *IEEE Antennas Wireless Propag. Lett.*, vol. 9, pp. 1092–1095, 2010.
[10] N. K. Das, T. Inoue, T. Taniguchi, and Y. Karasawa, "An experiment on MIMO system having three orthogonal polarization diversity branches in multipath-rich environment," in *Proc. 60th Veh. Technol. Conf.*, Sep. 2004, pp. 1528–1532.
[11] J. Sarrazin, Y. Mahe, S. Avrillon, and S. Toutain, "Investigation on cavity/slot antennas for diversity and MIMO systems: The example of a three-port antenna," *IEEE Antennas Wireless Propag. Lett.*, vol. 7, pp. 414–417, 2008.
[12] N. Honma, K. Nishimori, Y. Takatori, A. Ohta, and S. Kubota, "Proposal of compact MIMO terminal antenna employing Yagi–Uda array with common director elements," in *Proc. IEEE Int. Symp. Antenna Propag.*, Jun. 2007, pp. 2405–2408.
[13] C. B. Dietrich, K. Dietze, J. R. Nealy, and W. L. Stutzman, "Spatial, polarization, and pattern diversity for wireless handheld terminals," *IEEE Trans. Antennas Propag.*, vol. 49, no. 9, pp. 1271–1281, Sep. 2001.
[14] R. B. Bakar and H. Arai, "Three layers switched multibeam antenna with dual-polarization," in *Proc. IEEE Int. Workshop Electromagn. (iWEM)*, Aug. 2014, pp. 167–168.
[15] *CST—Computer Simulation Technology*. Accessed: Oct. 26, 2016. [Online]. Available: https://www.cst.com/
[16] K. Takahashi, R. Bakar, H. Arai, T. Ihara, and Y. Ishikawa, "Design of four elements MIMO antenna using the theory of characteristic mode," in *Proc. Int. Symp. Antenna Propag. (ISAP)*, Oct. 2016, pp. 232–233.
[17] G. J. Foschini, "Layered space-time architecture for wireless communication in a fading environment when using multi-element antennas," *Bell Labs Tech. J.*, vol. 1, no. 2, pp. 41–59, 1996.
[18] Hyper Physics. *Fresnel Equation*. Accessed: Apr. 25, 2016. [Online]. Available: http://hyperphysics.phy-astr.gsu.edu/hbase/phyopt/freseq.html
[19] EEM Inc. *EEM-RTM Manual*. Accessed: Oct. 26, 2016. [Online]. Available: http://www.e-em.co.jp/rtm/eem_rtm.htm

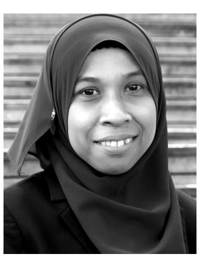

Bakar Rohani (M'13) was born in Malaysia. She received the B.E. degree in communication and computer from Universiti Kebangsaan Malaysia, Malaysia, in 2004, and the M.S. degree in telecommunication and information engineering from Universiti Teknologi MARA, Malaysia, in 2012, and the Dr.Eng. degree in physics, electrical and computer from Yokohama National University (YNU), Yokohama, Japan, in 2016.

From 2004 to 2012, she was with Hitachi Electronics and Products, Malaysia, as an Engineer in quality analysis and control for Hitachi Media Electronic Japan. Since 2016, she has been an Assistant Professor with the Division of Physics, Electrical and Computer Engineering, Graduate School of Engineering, YNU. Her current research interests include MIMO antenna system, array antenna design, channel capacity, small base station antenna, and characteristic mode analysis.

Dr. Rohani is a member of Institute of Electronics, Information and Communication Engineers.

Kanata Takahashi was born in Hachiouji, Japan, in 1992. He received the B.E. and M.E. degrees in physics, electrical and computer from Yokohama National University (YNU), Yokohama, Japan, in 2015 and 2017, respectively.

He is an Engineer with the Developing Department, NEC Co., Kawasaki, Japan. His current research interests include MIMO antenna system, array antenna design, and channel capacity.

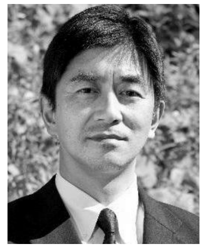

Hiroyuki Arai (F'12) received the B.E. degree in electrical and electronic engineering and the M.E. and D.E. degrees in physical electronics from the Tokyo Institute of Technology, Tokyo, Japan, in 1982, 1984, and 1987, respectively.

He was a Research Associate with the Tokyo Institute of technology. In 1989, he joined Yokohama National University, Yokohama, Japan, as a Lecturer. He was a Visiting Scholar with the University of California at Los Angeles, Los Angeles, CA, USA, in 1997. He was a Visiting Professor in 2005 and an Adjunct Professor from 2012 to 2014, respectively, with Yonsei University, Seoul, South Korea. He is currently a Professor with the Department of Electrical and Computer Engineering, Yokohama National University. He investigated microwave passive components for high-power handling applications, such as RF plasma heating in large tokamaks. He developed a flat diversity antenna for mobile telephone terminal, a polarization diversity base station antenna for Japanese PDC systems, small base station antennas of in-building microcellular system, and direction-of-arrival (DOA) estimation for cellular system. He has authored or co-authored five edited books, three research book chapters, over 140 journal papers, and 1100 conference papers. His current research interests include multiple-input and multiple-output antennas, wireless power transmission, energy harvesting in EM waves, and electromagnetic compatibility/electromagnetic interference antennas.

Prof. Arai is a Fellow of the Institute of Electronics, Information and Communication Engineers (IEICE). He received the Young Engineers Award from the IEICE of Japan in 1989, and the Meritorious Award on Radio by the Association of Radio Industries and Businesses in 1997 for the development of polarization diversity antenna, in 2006 for the development of DOA estimation system, and in 2011 for the development of light weight phantom. He was the Editor-in-Chief of the IEICE Transactions on Communications from 2005 to 2007, and the Chair of the IEEE AP-S Japan Chapter from 2009 to 2010. He was an Associate Editor of the IEEE TRANSACTIONS ON ANTENNAS AND PROPAGATION from 2011 to 2013, and the Chair of the Technical Group on Antennas and Propagation of IEICE from 2013 to 2014.

Yasuko Kimura received the B.E. degree from Tokai University, Tokyo, Japan, in 1998, and the M.E. degree from Tsukuba University, Tsukuba, Japan, in 2000.

In 2000, she joined the NTT DOCOMO, Inc., Yokosuka, Japan, and since then, she has been involved in the research and development of base station antennas for mobile radio communications, where she is now an Assistant Manager with the Radio Access Network Development Department.

Taisuke Ihara received the B.S. degree from the Tokyo University of Science, Tokyo, Japan, in 1992, and the M.S. and Dr.Eng. degrees from Tohoku University, Sendai, Japan, in 1994 and 2003, respectively.

In 1994, he joined NTT Mobile Communications Network, Inc. (now NTT DOCOMO, Inc.), Yokosuka, Japan, since then, he has been involved in the research and development of base station antennas.

Dr. Ihara received the Japan Young Engineer Award from IEICE Japan in 2001.